COMPARISON OF KAOLIN AND KAOLINITIC CLAYSTONES AS RAW MATERIALS FOR PREPARING METAKAOLINITE-BASED GEOPOLYMERS

#PETR KOUTNÍK, ALEŠ SOUKUP, PETR BEZUCHA, JAN ŠAFÁŘ, PAVLÍNA HÁJKOVÁ, JIŘÍ ČMELÍK

*Unipetrol Centre for Research and Education, Revoluční 1521/28,
40001 Ústí nad Labem, Czech Republic*

#E-mail: petr.koutnik@unicre.cz

One kaolin and two kaolinitic claystones were characterised (XRD, XRF, FTIR, TG, SEM, MIP), dehydrated at 750 °C, finely ground and mixed with an alkali activator in weight ratios of 55:80, 55:75, 60:70, 65:65, 70:60 and 75:55. Geopolymer binders were then prepared by water addition up to an invariable content of 34 wt. %. The binders were finally mixed with quartz sand in a weight ratio of 40:60. The differences in the properties between the two types of clay materials, the changes in these properties due to dehydration and milling, and the impact of the observed differences on the properties of the geopolymer binders (dynamic viscosity, pore size distribution, colour shade) and filled geopolymers (flexural strength, compressive strength, elastic modulus) were investigated. The kaolinitic claystones had a morphology different from the kaolin, characterised by smaller kaolinite plates, significantly lower pore volumes with average pore diameters and a higher impurities content that caused a more intense colour compared to the kaolin. The above-mentioned differences remained unchanged after thermal and mechanical treatment of the starting clay materials. The geopolymer binders prepared from the calcined and milled kaolinitic claystones were darker in colour and had a significantly lower dynamic viscosity (approximately three times) compared to the geopolymer binders prepared from the kaolin. The dynamic viscosity decreased with the decreasing activator content, while the volume and pore size increased. The mechanical properties of all the prepared geopolymers were excellent (compressive strength >50 MPa, bending strength > 7.9 MPa and elastic modulus >15 GPa) up to a ratio of metakaolinite component/alkali activator of 1:1.

INTRODUCTION

Geopolymers are materials based on the alkaline activation of aluminosilicates. Powdered aluminosilicates are partially soluble in a liquid alkaline activator, typically in an alkali metal hydroxide water solution or a liquid alkali silicate (water glass), and free aluminosilicate and silicate oxides are formed in the polymeric form by a polycondensation reaction. The effect of this reaction is the hardening of a geopolymer binder [1]. Geopolymer binders are usually filled or reinforced by various solid materials in order to improve their properties and/or to reduce the price similarly to other binder systems [2, 3].

Geopolymers exhibit good mechanical properties, resistance to high temperatures and chemicals: especially to acids and organic solvents. Geopolymer properties depend on the sort of aluminosilicate, the type of alkali cation (usually Na^+ or K^+) [4, 5], Si/Al molar ratio [6-8], the Si/Na molar ratio [9-14], water content [15-19] and the curing conditions [17, 20-23]. Some geopolymer properties can be modified by additives. Geopolymers can be coloured [24], the setting time can be accelerated by calcium ions [25] and the viscosity

of the geopolymer binders can be lowered by adding plasticisers [16, 26, 27]. Geopolymer properties and their variability enable applications in many industrial fields. New building materials [16, 28], coatings resistant to high temperatures [29, 30], fibre composites [31, 32], materials for the restoration of monuments [33], catalysts [34, 35], sorbents [36, 37] and materials for waste immobilisation [22, 38] have been developed on the basis of geopolymers.

The properties of the solid component have significant influence on the process of geopolymerisation, especially the ability of aluminosilicate to dissolve in an alkaline activator. The solid components, however, directly influence the physical properties, since the undissolved residue is inbuilt as a part of the resulting geopolymer. The applications of many various sources of Al and Si for geopolymer preparation have been investigated – rice husk ash, demolition wastes, blast furnace slag, volcanic ash, etc. [13, 14, 39-41]. Nevertheless, the most popular solid raw materials are fly ashes and metakaolin, because they can provide geopolymers with excellent properties and are available worldwide in sufficient quantities for industrial production. Fly ash is a cheap, darkly shaded, fine powder

material generated during coal combustion in thermal power plants. The particle size distributions, chemical and mineralogical compositions of fly ashes are variable because they strongly depend on the coal quality and combustion conditions. In contrast, commercial meta-kaolins are more expensive, lightly shaded with a generally similar composition and guaranteed particle size distribution. They are manufactured by the calcination of purified kaolin with high kaolinite content under controlled conditions [42, 43]. In the process, kaolinite is dehydroxylated to meta-kaolinite. Metakaolins are produced on an industrial scale primarily as pozzolans, i.e., materials able to bind $Ca(OH)_2$ and, thereby, improve the properties of building materials based on Portland cement [44].

The aim of this comparative study is the preparation of metakaolinite-rich materials by the calcination of different clay raw materials (kaolin or kaolinitic claystones), the characterisation of the prepared metakaolinite components and the investigation of the link between their properties and the properties of metakaolinite-based geopolymers, prepared equally under standardised conditions.

EXPERIMENTAL

Materials

The raw materials used for the preparation of metakaolinite components were commercial products: purified, granulated kaolin KDG from the locality of Hlubany (Kaolin Hlubany, a.s., Czech Republic), and natural kaolinitic claystones W Supra from the locality of Vyšehořovice and $D_{3,5}$ from the locality of Rynho-lec-Hořkovec (both from České lupkové závody, a.s., Czech Republic). The granularity of the claystones was below 0 - 20 mm. The samples of the materials were labelled in the above-mentioned order as C1 to C3. The sodium silicate (Vodní sklo, a.s., Czech Republic) and sodium hydroxide pellets (Lach-Ner, s.r.o., Czech Republic) were used for the preparation of the alkali activator. Quartz sand of grain size 0 - 2 mm (Provodínské písky, a.s., Czech Republic) was added as a filler for the preparation of the geopolymers that were used for the testing of the mechanical properties. The chemical compositions of the raw materials are given in Table 1.

Analytical and testing methods

The chemical compositions of the clay materials were determined by X-ray fluorescence (BRUKER S8 Tiger).

An inductively coupled plasma optical emission spectrometer OPTIMA 8000 (Perkin Elmer) was used to determine the content of the micro-elements and the K/Na ratio in the liquid sodium silicate. The total contents of the alkali metals (Na, K) and of SiO_2 in the sodium silicate were determined by conventional acid-base titration methods; the reason for their application being the higher accuracy at higher concentrations compared to other methods.

A BRUKER D8 Advanced X-Ray diffraction system (XRD) equipped with a BRUKER SSD 160 detector and operating with Cu-Kα radiation at 40 kV and 25 mA was used for the analysis of the clay materials and metakaolinite components. XRD scanning was taken at the step $2\theta = 0.02$ over an angular range from 5° to 70° with a 1 s counting time.

The thermal analysis of the clay materials (TG, DTA) was performed using a Discovery Series thermal analysis system from TA Instruments. The samples were heated at a heating rate of 10 °C·min⁻¹ up to 1000 °C in flowing nitrogen (20 ml·min⁻¹).

The morphology of the clay materials and metakaolinite components was studied by a scanning electron microscope Mira 3 from TESCAN.

A Mastersizer 2000 laser diffraction particle size analyser (MALVERN Instruments) was used to determine the size distribution of the prepared metakaolinite components. The agglomerates were disrupted by ultrasound treatment.

Table 1. The chemical composition (wt. %) of the raw materials.

	H₂O	SiO₂	Al₂O₃	Fe₂O₃	CaO	MgO	Na₂O	K₂O	TiO₂
C1	–	53.3	32.6	0.52	0.13	0.38	–	0.61	0.36
C2	–	46.3	37.3	0.78	0.17	0.12	–	0.81	1.47
C3	–	47.4	34.8	3.05	0.27	0.27	–	1.30	1.08
sodium silicate	53.8	29.7	0.10	0.01	–	–	16.2	0.18	–
sand	–	99.0	0.48	–	–	–	-	0.22	–

	P₂O₅	V₂O₅	Cr₂O₃	ZrO₂	SrO	BaO	ZnO	Cl	SO₃	LOI*
C1	0.02	–	–	-	–	–	0.01	0.02	0.06	11.96
C2	0.07	0.04	0.02	0.03	0.01	-	0.02	–	0.30	12.56
C3	0.17	–	0.01	–	–	0.09	0.01	–	0.04	11.38
sodium silicate	–	–	–	–	–	–	–	–	–	–
sand	–	–	–	–	–	–	–	–	–	0.12

* LOI = Loss on ignition

The pore size distributions were determined using AutoPore IV 9510 mercury intrusion porosimetry (Micromeritics), which operates with pressures from 0.01 MPa to 414 MPa. A region was evaluated, quantitatively corresponding to the pore size of 4 - 10 000 nm for the clay materials and 4 - 350 000 nm for the geopolymer binders (full measurement range).

The FTIR spectra were taken using a Nicolet 380 FTIR spectrometer in the transmittance mode. The wave number range was 400 - 4000 cm^{-1} at a resolution of 4 cm^{-1}. KBr tablets containing 1.64 wt. % of the sample were measured.

The specific gravity was determined by the pycnometric method.

The dynamic viscosities of the geopolymer binders were measured by a rotary rheometer Rheotest 2 (Rheotest Medingen) at 25 °C using a 32.4 mm diameter cylinder at a shear rate of 72.9 s^{-1}.

A universal testing machine, LabTest 6.200 (Labortech) was used for the determination of the mechanical properties. The flexural strength was determined using a three-point-bending test on three samples (20 × 20 × 160 mm) with a crosshead speed of 0.1 MPa·s^{1} (ca. 0.25 mm·min^{-1}). The compressive strength and modulus of elasticity were measured according to the ISO 1920-10 standard on six prismatic samples (30 × 30 × 64 mm) with a crosshead speed of 0.5 MPa·s^{-1} (ca. 0.25 mm·min^{-1}). The mechanical properties were determined 7 days after the sample preparation.

Thermal and mechanical treatment of kaolin and kaolinitic claystones

The starting materials were dehydrated at a temperature of 750 °C in an electric furnace for 15 min. Selection of the calcination conditions was based on the results of the thermogravimetric analysis of the C1-C3 clay materials. The internal volume of the furnace was 50 l and the batch weight was 5 kg. The heating time was controlled according to the temperature measured

Figure 1. The heating curves during the dehydration of the starting clay materials.

with a sensor placed inside the material: the heating was stopped 15 minutes after reaching 750 °C. The material was allowed to cool down very slowly (overnight) inside the furnace. The typical heating curves are shown in Figure 1. The dehydrated clay materials were labelled as C1C-C3C.

The dehydrated clay materials (charge 8.2 kg) were ground in a 250 l ball mill with 45 kg of manganese steel grinding balls (diameter from 16 to 40 mm) at 35.4 rpm for 6 h. The ground materials were classified by using a 50 ATP air classifier from Hosokawa Alpine and labelled as C1M-C3M.

Preparation of geopolymers

The common alkali activator with a silicate modulus SiO$_2$:Me$_2$O (Me = Na + K) of 1.39 and the H$_2$O content of 56.61 % was prepared by dissolving the solid sodium hydroxide in a commercial sodium silicate solution and the addition of distilled water. This composition of an alkali activator has been successfully applied in the geopolymers' preparation [23].

The C1M-C3M metakaolinite components were dried at 110 °C in order to remove the water absorbed during the milling and storage. The geopolymer binders were then obtained by mixing the metakaolinite components with an alkali activator in a planetary mixer at room temperature for 10 min; distilled water was then added to achieve a total water content of 34 % in the geopolymer binder and mixing continued for 5 min. The weight ratios of the metakaolinite component to the alkali activator were 55:80, 55:75, 60:70, 65:65, 70:60 and 75:55 for all the C1M-C3M metakaolinite components. The geopolymer binders were labelled as G1-G18. The obtained compositions are given in Table 2. The dynamic viscosity was determined immediately after blending. The mixtures of the metakaolinite components with the alkali activator were liquid, except only for three G4-G6 geopolymer binders prepared from the C1M metakaolinite component with the alkali activator, which were plastic (G4), or the mixture granulated (G5 and G6). The time of the mixing with the distilled water was, in these three cases, prolonged by another 5 minutes, which led to a return to liquid consistency.

The geopolymer binders were finally mixed up with quartz sand in a weight ratio 40:60 for 5 minutes, and the homogenous mixtures were poured into silicon moulds. Air bubbles were removed by 5-minute vibration, the moulds were put in sealed polyethylene bags and cured at 60 °C in an electric oven. The samples were taken out of the oven after 4 h, de-moulded and left to cure at an ambient temperature (20 °C) for 7 days. The curing conditions, including the time, were chosen on the base of the results of Rovnaník [23], which confirms that the samples cured under the described conditions reach the final strengths.
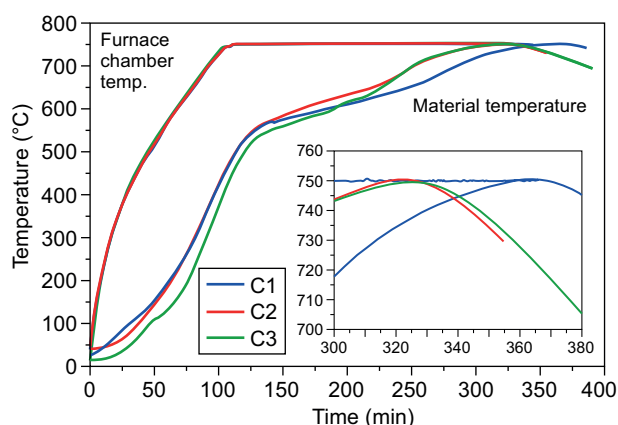
Table 2. The composition of the geopolymer binders (g).

Raw material	G1	G2	G3	G4	G5	G6	G7	G8	G9
C1M	55	55	60	65	70	75	–	–	-
C2M	–	–	–	–	–	–	55	55	60
C3M	–	–	–	–	–	–	–	–	-
alkali activator	80	75	70	65	60	55	80	75	70
H_2O	0.9	2.6	6.9	11.2	15.5	19.8	0.9	2.6	6.9
Si/Al (mol/mol)	2.16	2.11	2.00	1.91	1.83	1.76	1.75	1.71	1.61
Me*/Al (mol/mol)	1.21	1.14	0.98	0.84	0.73	0.63	1.08	1.01	0.87
H_2O/Al (mol/mol)	6.40	6.25	5.92	5.64	5.39	5.19	5.70	5.56	5.26
H_2O (wt. %)	34.0	34.0	34.0	34.0	34.0	34.0	34.0	34.0	34.0
C/activator** (g/g)	0.69	0.73	0.86	1.00	1.17	1.36	0.69	0.73	0.86

Raw material	G10	G11	G12	G13	G14	G15	G16	G17	G18
C1M	–	–	–	–	–	–	–	–	–
C2M	65	70	75	–	–	–	–	–	–
C3M	–	–	–	55	55	60	65	70	75
alkali activator	65	60	55	80	75	70	65	60	55
H_2O	11.2	15.5	19.8	0.9	2.6	6.9	11.2	15.5	19.8
Si/Al (mol/mol)	1.53	1.45	1.39	2.04	1.99	1.88	1.79	1.71	1.64
Me*/Al (mol/mol)	0.75	0.65	0.56	1.21	1.14	0.98	0.84	0.73	0.63
H_2O/Al (mol/mol)	5.01	4.80	4.61	6.32	6.16	5.84	5.56	5.32	5.11
H_2O (wt. %)	34.0	34.0	34.0	34.0	34.0	34.0	34.0	34.0	34.0
C/activator** (g/g)	1.00	1.17	1.36	0.69	0.73	0.86	1.00	1.17	1.36

* Me = Na + K, ** metakaolinite component/alkali activator ratio

RESULTS AND DISCUSSION

Properties of kaolin and kaolinitic claystones

The chemical analyses of the raw materials are given in Table 1. The C2 and C3 kaolinitic claystones contained less SiO_2 and more Al_2O_3 and impurities, especially TiO_2 and Fe_2O_3, compared to the C1 kaolin. The highest Fe_2O_3 (3.05 wt. %) content was found in the sample C3, which was the main reason for its dark shade (Figure 2).

Figure 2. The appearance of the kaolin and kaolinitic claystones before (left column) and after the thermal treatment (column C), after the thermal and mechanical treatment (column M), the geopolymer binders (column G) and the filled geopolymers (column GS).

The XRD patterns of the C1-C3 samples are reproduced in Figure 3. The major phase in all the samples was kaolinite, the minor phases were quartz and illite. The intensity of the kaolinite signal was much lower for the C2 and C3 claystones compared to the C1 kaolin under the same measuring conditions.

The FTIR spectra of the C1-C3 clay materials are given in Figure 4, and their interpretation is summarised in Table 3. All three spectra were almost the same, typical for kaolinite [45-48]. They showed four well-defined OH group bands in the 3700 - 3600 cm⁻¹ region. The intensities of the bands at 3619 cm⁻¹ were higher than that of the bands at 3697 cm⁻¹ for all the tested clay materials. According to Tironi et al. [47], this means the kaolinite had a well-ordered structure. The intense absorption bands occurring at 1115, 1031 and 1007 cm⁻¹ belong to the Si–O stretching modes [46]. The bands at 940 and 941 cm⁻¹ indicated –OH bending vibrations that are mainly caused by Al–OH groups [45]. The bands at the frequencies of 798, 754, 697 and 536 cm⁻¹ were attributed to the Si–O and Al–O bending vibrations [49]. Another band at the frequency 468 cm⁻¹ was assigned to a T–O–T (T: Si or Al) bridge of aluminosilicates [45] and the last band with the lowest frequency of 428 cm⁻¹ was related to the bending vibration of Si–O [48].

The results of thermogravimetric analysis of the C1-C3 samples are shown in Figure 5. The total weight losses were similar in all the clay materials in the narrow interval 11.71 - 12.60 wt. %. The TG (Thermal Gravimery) curves were typical for the transformation of kaolinite to metakaolinite [10, 50]. The peaks on

the DTA (Differential Thermal Analysis) curves representing the kaolinite dehydroxylation had an identical shape, but they were slightly shifted on the temperature axis, which likely points to a partly different character of disorders in the kaolinite structure and the contents and the kinds of impurities [10, 51].

The morphological difference among the C1-C3 samples were documented on an SEM. All the clay
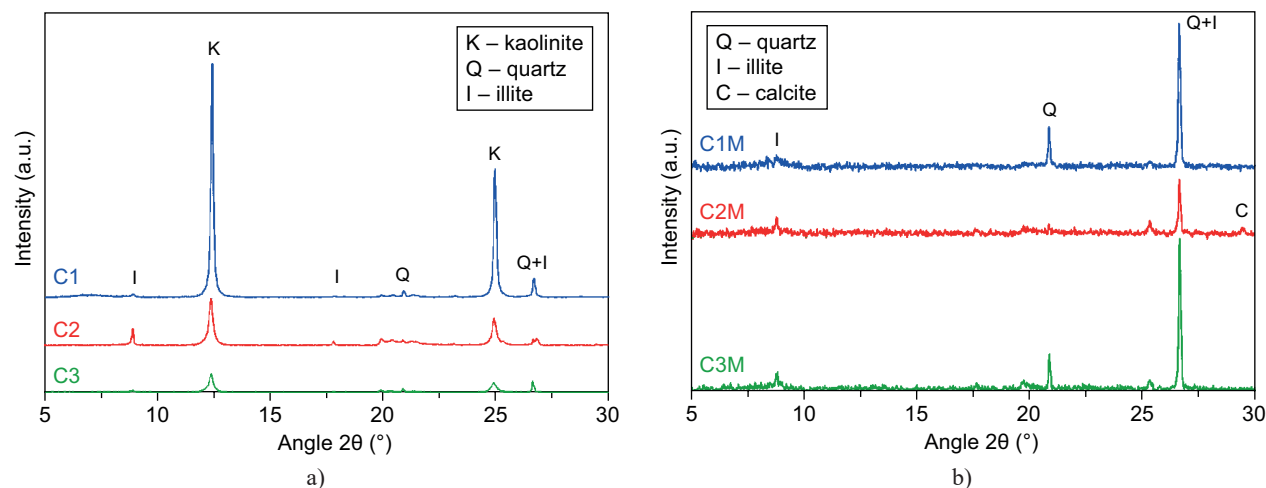

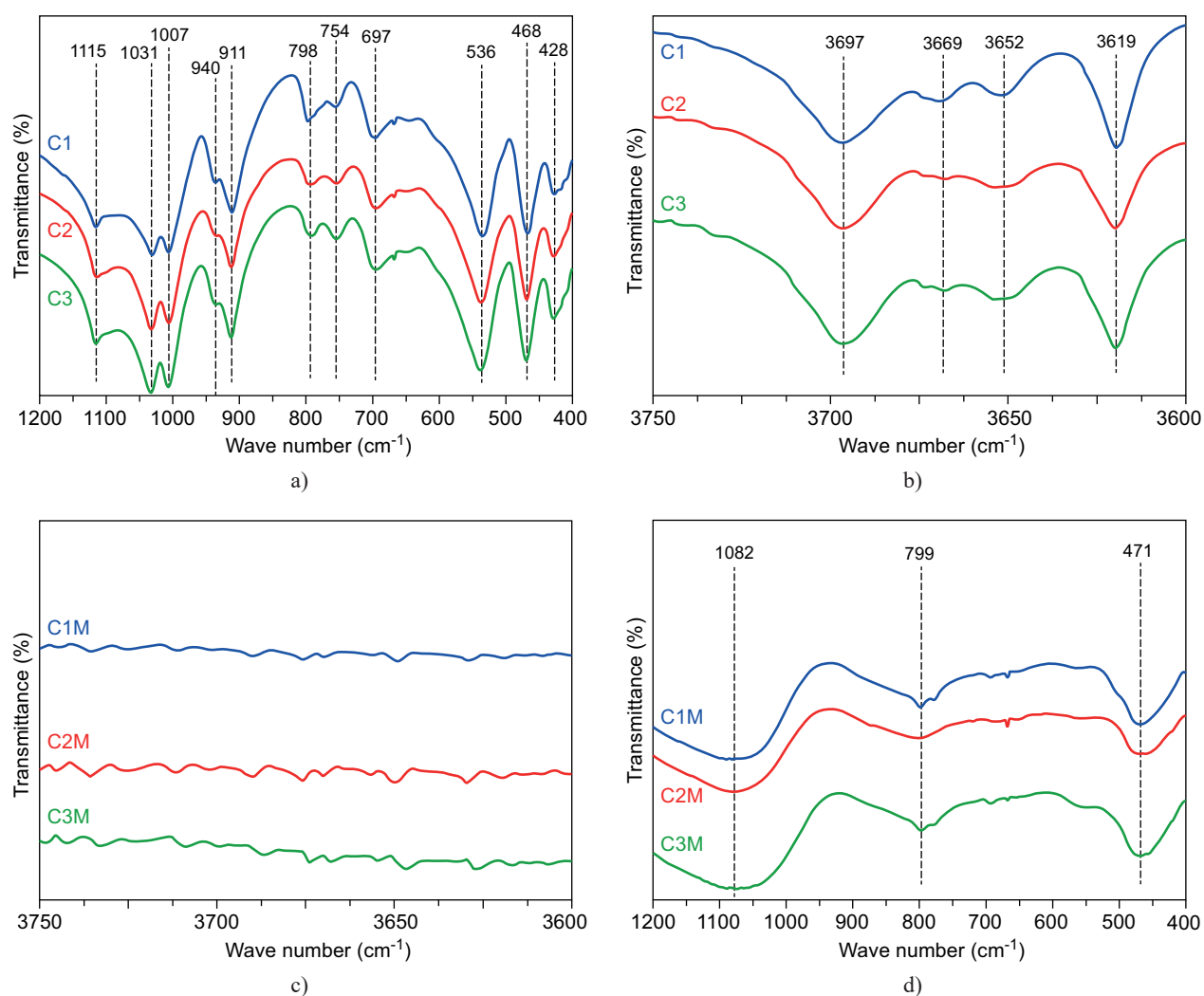Figure 3. The XRD patterns of the clay materials before (a) and after (b) the thermal and mechanical treatment.

Figure 4. The FTIR spectra of the clay materials before (a, b) and after (c, d) the thermal and mechanical treatment.

Table 3. The IR bands and their interpretation.

Samples	Absorption bands (cm^{-1})	Probable assignment
C1-C3	3697	O–H stretching vibration
	3669	O–H stretching vibration
	3652	O–H stretching vibration
	3619	O–H stretching vibration
	1115	Si–O stretching vibration
	1031	Si–O stretching vibration
	1007	Si–O stretching vibration
	940	Al–OH bending vibration
	911	Al–OH bending vibration
	798	Al–O, Si–O bending vibration
	754	Al–O, Si–O bending vibration
	697	Al–O, Si–O bending vibration
	536	Al–O, Si–O bending vibration
	468	T–O–T (T: Si or Al) bending vibration
	428	Si–O bending vibration
C1M-C3M	1082	Si–O stretching vibration (amorphous SiO_2)
	799	Al(IV)–O bending vibration
	471	T–O–T (T: Si or Al) bending vibration
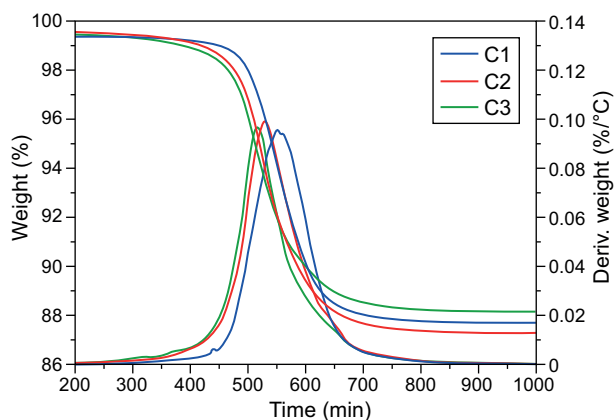
Figure 5. The thermal analysis curves of the clay materials.

materials samples contained typical kaolinite plates [10, 51]. A significant difference between the kaolin and claystones resided, however, in the size and level of the order in these plates. While the kaolinite plates in the sample of the C1 kaolin were large and mostly arranged in a parallel fashion, the plates in the C2 and C3 claystones were significantly smaller and structured disorderly, as shown in Figure 6.

The physical properties of the C1-C3 samples are given in Table 4, the appearance is shown in Figure 2 and the pore size distributions are shown in Figure 7. The C1 kaolin had a white colour, the C2 claystone was light grey and the C3 claystone was brown. All the clay materials had almost the same specific gravity, which was expected as a result of the similar mineralogical nature. The differences in the pore distribution between the kaolin and claystones was determined by mercury intrusion porosimetry, with a pore size interval of 4 - 10 000 nm. The C1 kaolin mainly contained macropores (pore size > 50 nm), while the C2 and C3 claystones also contained a significant portion of mesopores (pore size 2 - 50 nm), as shown in Figure 7. A higher content of macro-pores in the C1 sample was reflected by significantly higher pore volumes and average pore diameters in comparison with the C2 and C3 claystones (Table 4).

The reason for the significant differences in the physical properties of the kaolin and kaolinite clays are the different conditions at their origin. These differences partially persist after the calcination, as shown below.

Properties of thermal and mechanically treated kaolin and kaolinitic claystones

The C1M-C3M metakaolinite components were prepared by calcination, grinding and classification of the starting C1-C3 clay materials. The chemical composition of the C1M-C3M samples, which is shown in Table 5, indicated a slight, very similar increase in the iron content in all the samples during the treatment, most likely due to the abrasion of the grinding balls. The C1M and C2M samples were also slightly contaminated

Table 4. The physical properties of the clay materials before and after the thermal and mechanical treatment.

	Specific gravity (kg·m^{-3})	Bulk density (kg·m^{-3})	Pore parameters		Particle size	
			V (mm^3·g^{-1})*	R (nm)**	d$_{50}$ (μm)	d$_{90}$ (μm)
C1	2593	–	351	217	–	–
C2	2613	–	161	80	–	–
C3	2621	–	182	79	–	–
C1C	–	–	502	238	–	-
C2C	–	–	144	54	–	–
C3C	–	–	152	46	–	–
C1M	2459	331	890	338	4.57	15.21
C2M	2559	475	715	291	4.08	11.65
C3M	2569	454	707	221	4.35	14.12

* V = pore volume; ** R = average pore diamer

by calcite (< 4 wt. % in the case of C2M and < 1 wt. % in the case of C1M), as evidenced by the increase in CaO content compared to the C1 and C2 samples and the XRD analysis results (Figure 3). These contaminations, however, could not affect the subsequent set of geopolymers properties, thanks to only a small amount and the relatively inert nature of these impurities [52]. The reason for the contamination was probably an insufficient cleaning of the mill before the milling of the calcinates.

The results of the XRD and FTIR analyses, shown in Figure 3 and 4, demonstrated the complete transformation of the crystalline kaolinite to the amorphous metakaolinite during calcination in all the clay materials. The XRD patterns of the C1M-C3M samples did not exhibit the characteristic peaks of kaolinite, but also showed the presence of some impurities (quartz and illite in all samples and calcite in the case of the C2M sample). The FTIR spectra of the C1M-C3M samples were almost identical and corresponded to the

a) C1

b) C1M

c) C2

d) C2M

e) C3

f) C3M
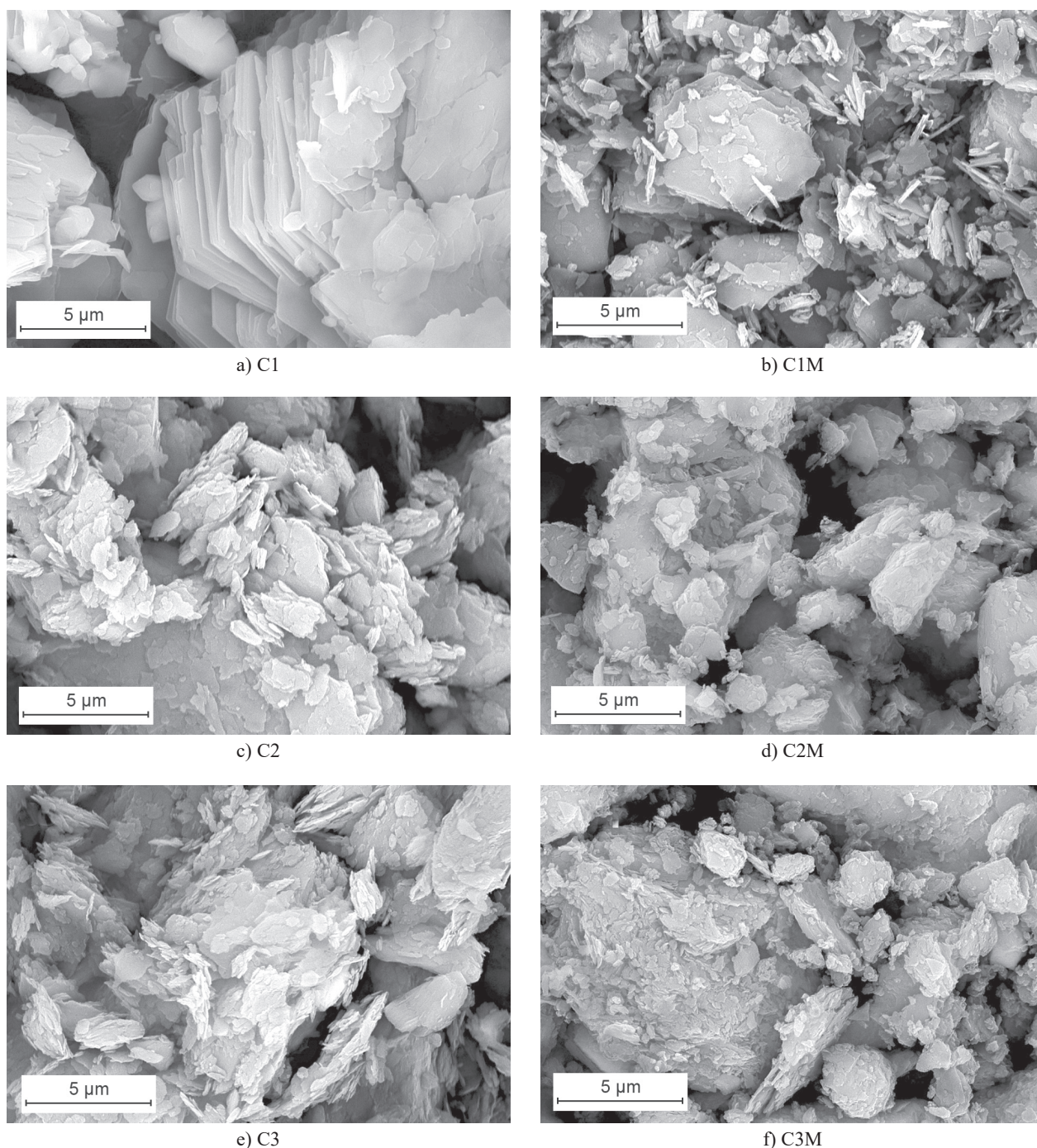
Figure 6. The morphology of the clay material particles before and after the thermal and mechanical treatment.

spectra of metakaolinite. The spectra contained a band at 1082 cm^{-1} attributed to the stretching vibrations in the amorphous SiO_2, a band at 799 cm^{-1} related to an AlO_4 tetrahedron, and a band at 471 cm^{-1} indicating a T–O–T (T: Si or Al) aluminosilicate bridge [45, 47]. The OH group bands observed in the FTIR spectra of the C1-C3 clay materials (region 3600 - 3700 cm^{-1}, bands 940 and 911 cm^{1}) totally disappeared.
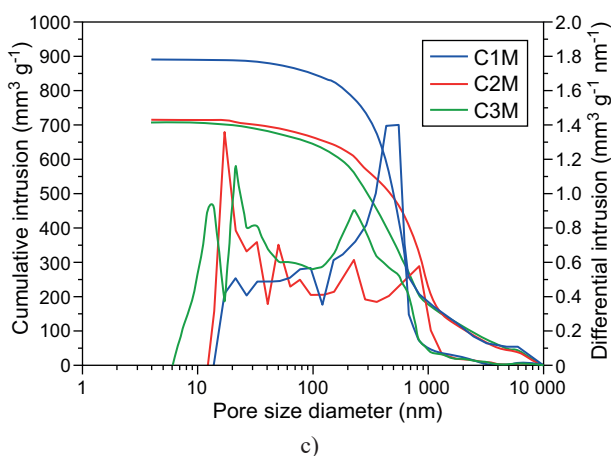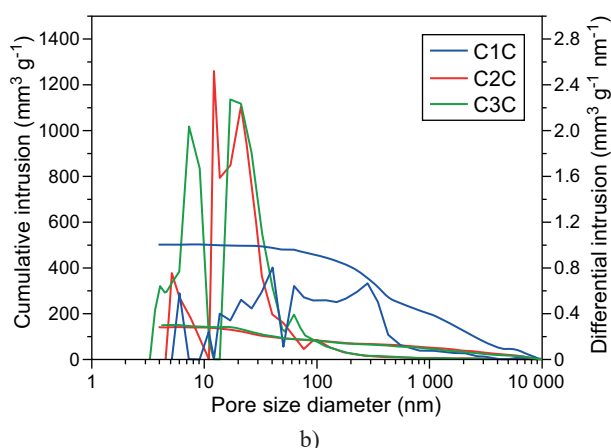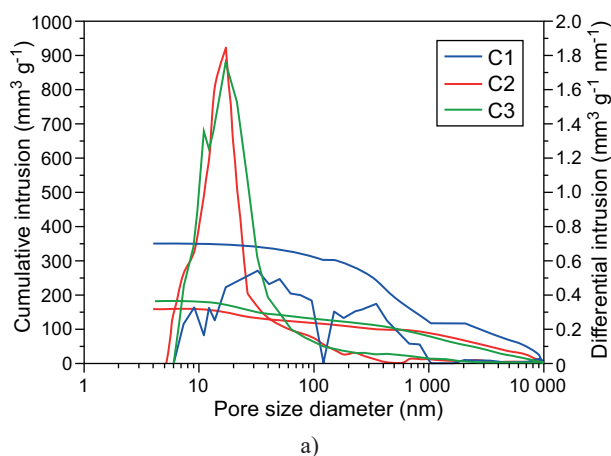
The parameters of the particle size distribution of the C1M-C3M milled samples, determined by laser diffraction, are given in Table 4. All the samples had a similar particle size distribution expressed by the values of d_{50} and d_{90} that were in the narrow intervals of 4.08 - 4.57 μm (d_{50}) and 11.65 - 15.21 μm (d_{90}). These parameters were, thus, comparable to or even exceeded the values of the high quality metakaolins produced on an industrial scale and widely used for the preparation of geopolymers [23, 53, 54].

The morphology of the particles of C1M sample prepared from the C1 kaolin differed from the particle morphology of the C2M and C3M samples prepared from the C2 and C3 kaolinite claystones, as shown in Figure 6. The typical lamellar structure of kaolinite was preserved in all the samples during the thermal and mechanical treatment, but the C1M sample contained much more particles with a high aspect ratio compared to C2M and C3M samples. The reason was in the different particle morphology of the starting materials. Large one-directionally oriented plates were separated more readily during grinding then small and less structured plates.

The physical properties of the C1M-C3M samples are given in Table 4, their appearance is shown in Figure 2, the pore size distributions are shown in Figure 7 and the particle size distributions are shown in Figure 8 The C1M sample had a light beige colour, the C2M sample was light grey and the C3M sample was reddish brown due to a high Fe_2O_3 content. Calcination resulted in a decrease in the specific gravity by about 2 % for the C2M and C3M samples, and by about 5 % for the C1M sample. Generally, four processes could have an impact on the specific gravity change: dehydroxylation (mass reduction), oxidation of impurities (mass growth), shrinkage related to dehydroxylation (volume reduction) and expansion resulting from the α – β quartz transformation (volume growth) [55]. The specific pore volumes and average pore diameters of the thermally treated non-milled C1C kaolin, determined by mercury

Figure 7. The pore size distributions of the clay materials before (a) and after (b) the thermal treatment and after the thermal and mechanical treatment (c).
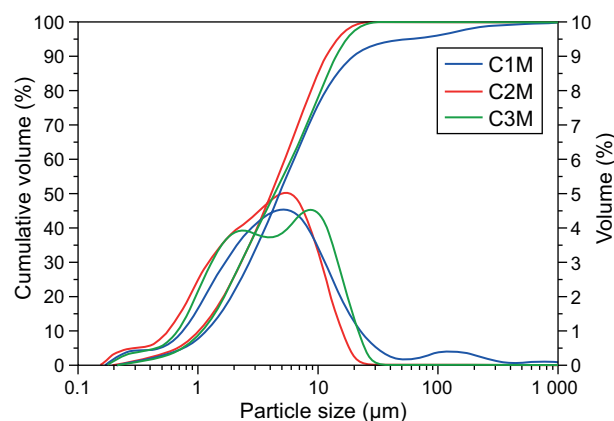

Figure 8. The particle size distributions of the clay materials after the thermal and mechanical treatment.

intrusion porosimetry, were slightly higher than the same characteristics of the raw C1 kaolin. On the contrary, the thermal treatment of the C2 and C3 claystones led to a slight decrease in the pore volumes and average pore diameters. Figure 7c depicts significant change in the pore distribution due to the milling of the thermally treated clay materials. The pore volumes and average

pore diameters of the thermally treated C1C-C3C samples significantly increased in the course of milling the C1M-C3M materials, probably due to the opening of the closed pores. The increase was especially high with the thermally treated C2M and C3M claystones with a factor of roughly 5 ×. The rise was much lower with the C1M treated kaolin, still the final pore volumes and average pore diameters of the C1M exceeded the parameters of the C2M and C3M samples values by 20 % to 30 %. The bulk densities of the C2M and C3M samples were similar and higher by about 40 % than the bulk density of the C1M sample, as a consequence of the described differences in the particle morphology and in the pore space.

Properties of geopolymer binders

The influence of the metakaolinite components/ alkali activator weight ratio on the dynamic viscosity of the geopolymer and binder was investigated for all three prepared metakaolinite components (C1M, C2M and C3M) as shown in Figure 9. The viscosity of the geopolymer binders prepared from the C2M and C3M samples was significantly lower in the region of the lower metakaolinite fraction (almost exactly 3 times),
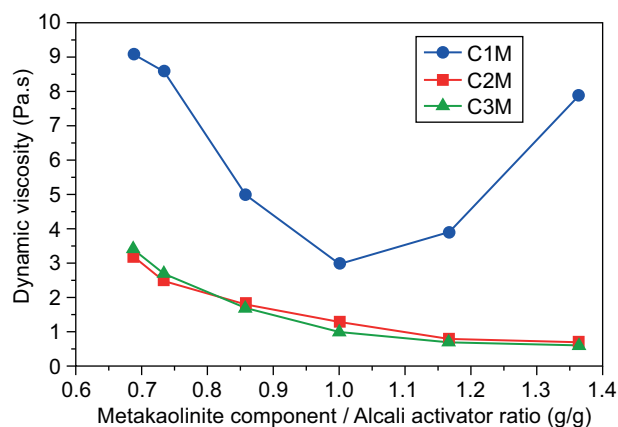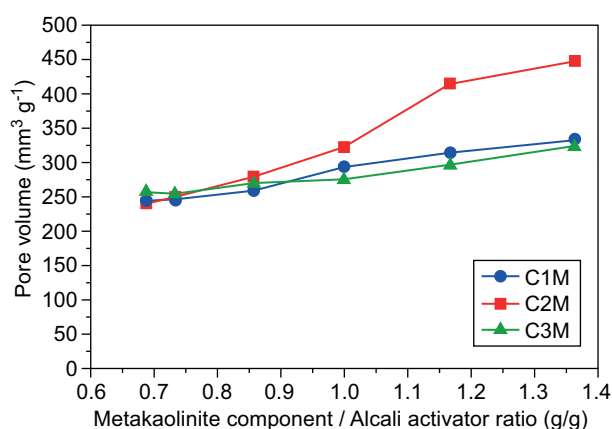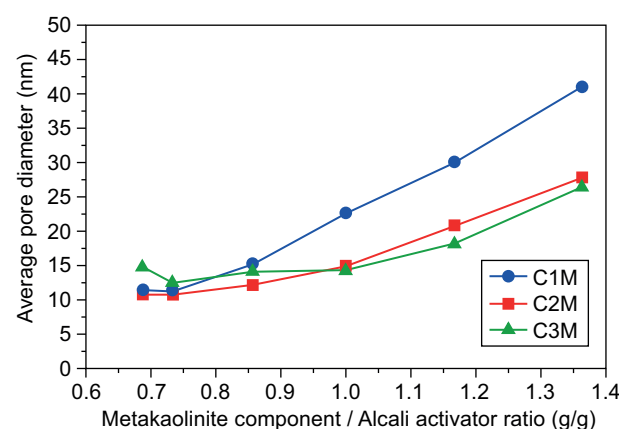
Figure 9. The influence of the metakaolinite components/alkali activator weight ratio on the dynamic viscosity of the geopolymer binders prepared from the C1M, C2M and C3M metakaolinite components.

Figure 10. The influence of the metakaolinite components/alkali activator weight ratio on the pore volume (a) and average pore diameter (b) of the geopolymer binders prepared from the C1M, C2M and C3M metakaolinite components.

Table 5. The chemical composition (wt. %) of the thermal and mechanically treated kaolin and kaolinitic claystones.

	SiO_2	Al_2O_3	Fe_2O_3	CaO	MgO	K_2O	TiO_2	P_2O_5	V_2O_5	Cr_2O_3
C1M	58.5	37.0	0.82	0.48	0.45	0.88	0.64	0.04	–	–
C2M	50.2	41.6	1.18	2.22	0.15	0.83	1.70	0.06	0.04	0.03
C3M	54.3	37.5	3.57	0.31	0.28	1.25	1.16	0.15	–	0.01

	ZrO_2	SrO	NiO	BaO	ZnO	MnO	CuO	Cl	SO_3	LOI*
C1M	0.01	–	–	–	0.01	–	-	0.04	0.08	0.97
C2M	0.02	0.01	0.01	0.03	0.01	0.01	0.01	–	0.26	1.57
C3M	–	0.02	–	0.07	–	–	0.01	–	0.04	1.32

* LOI = Loss on ignition

compared to the viscosity of the binders prepared from the C1M metakaolinite component. The difference could be caused by the different morphology of the particles, influencing the flow dynamics of the suspension. The second reason could be the lower volume of the solid phase in the geopolymer binders based on the C2M and C3M samples, because the C2M and C3M samples had a lower porosity and higher density compared to the C1M sample (Table 4). The lower volume of the solid phase in the suspension reduces the viscosity of the suspension according to the Krieg Dougherty Equation [56]. In the interval of metakaolinite component/alkali activator ratio less than 1, the dynamic viscosity of all freshly prepared binders decreased with the decreasing alkaline activator content, because both the SiO_2 and Na_2O contents in the binder decreased, but the total water content in the binder remained constant, as shown in Table 2. The unique course of the dependence shown in Figure 9 exhibiting a minimum viscosity with a metakaolinite component/alkali activator ratio of 1, was found in the geopolymer binders containing the C1M metakaolinite component. In this case, however, there could be an increase in the viscosity for the two samples with the lowest content of the activator (G5, G6), caused by the formation of the solid granules during the mixing of the activator with the metakaolinite component, which could affect the viscosity of the G5 and G6 geopolymer binders. An important finding resulting from the preparation of the geopolymer binders' observation was that the C2M and C3M samples could be used to prepare a liquid geopolymer binder with a significantly lower water content than by using the C1M sample.

The appearance of the hardened binders with the highest content of the metakaolinite component (G6, G12 and G18) are shown in Figure 2. The G6 sample had a light beige colour, the G12 sample was light brown and the G18 sample was reddish brown. The colour intensity increased in the order of G6 < G12 << G18, which reflected the increasing content of the impurities (especially Fe_2O_3) in the metakaolinite component.

The pore volume and average pore diameter in the hardened geopolymer binders were measured by means of a mercury intrusion porosimetry. The relationships between these key parameters and the metakaolinite component/alkali activator ratios are presented in Figure 10. Both the pore volume and average pore diameter increased with an increasing content of the metakaolinite component in the geopolymer binders. The mechanism can be explained in such a way that only a part of the porous particles of the aluminosilicate is dissolved during the alkali activation [57], and the pores of the undissolved residues are gradually filled with a geopolymer gel [23]. The increase in the pore volume and pore size can, therefore, be explained by an increase in the content of the undissolved residues of the metakaolinite component in the geopolymer binders. The type of the metakaolinite component did not have a signi-

ficant effect on the pore volume and pore diameter of the geopolymer binders up to a metakaolinite component/alkali activator ratio of 0.9. At higher ratios, these parameters were somewhat diverging, but without a specific link to the particular type of the metakaolinite component.

Mechanical properties of geopolymers

The mechanical properties of all the prepared geopolymers were excellent (compressive strength > 50 MPa, bending strength > 7.9 MPa and elastic modulus > 15 GPa) down to a ratio of the metakaolinite component/alkali activator of 1:1, a further decrease in the alkali activator content led to a decrease in the compressive strength and modulus of elasticity as shown in Figure 11. The obtained highest values of strengths resp. modulus were, within the experimental error, the same with the C3M and C1M metakaolinite components (compressive strength 69.4 MPa, flexural strength 10.5 MPa, elastic modulus 20.4 GPa resp. compressive strength 63.9 MPa, flexural strength 10.2 MPa, elastic modulus 19.8 GPa, respectively). The lower maximum strengths were observed with the geopolymers prepared from the C2M material (compressive strength 55.0 MPa, flexural strength 8.97 MPa, elastic modulus 18.0 GPa). The measured values were consistent with the published mechanical properties of the geopolymers of similar composition: compressive strength 55 - 70 MPa [3, 23, 26, 58-60], flexural strength 6 - 12 MPa [26, 58] and elastic modulus 14 - 24.4 GPa [58, 59].

The mechanical properties of the geopolymers depend on the chemical composition of the geopolymer binder, as the optimal composition of the metakaolin-based geopolymer binder had been reported with
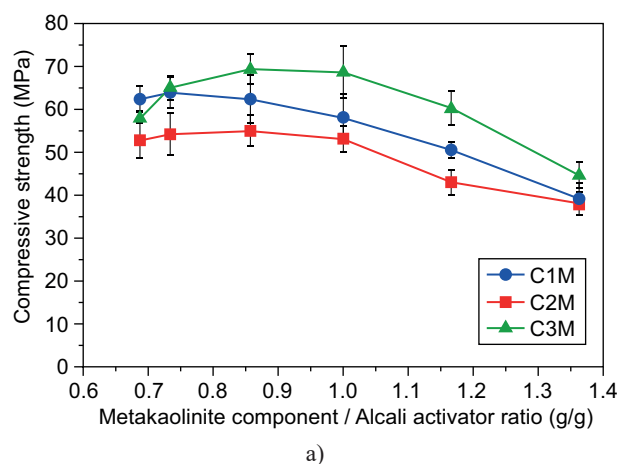

Figure 11. The influence of the metakaolinite components/ alkali activator weight ratio on the compressive strength (a) of the filled geopolymers prepared from the C1M, C2M and C3M metakaolinite components. The error bars represent the standard deviation. *(Continue on next page)*
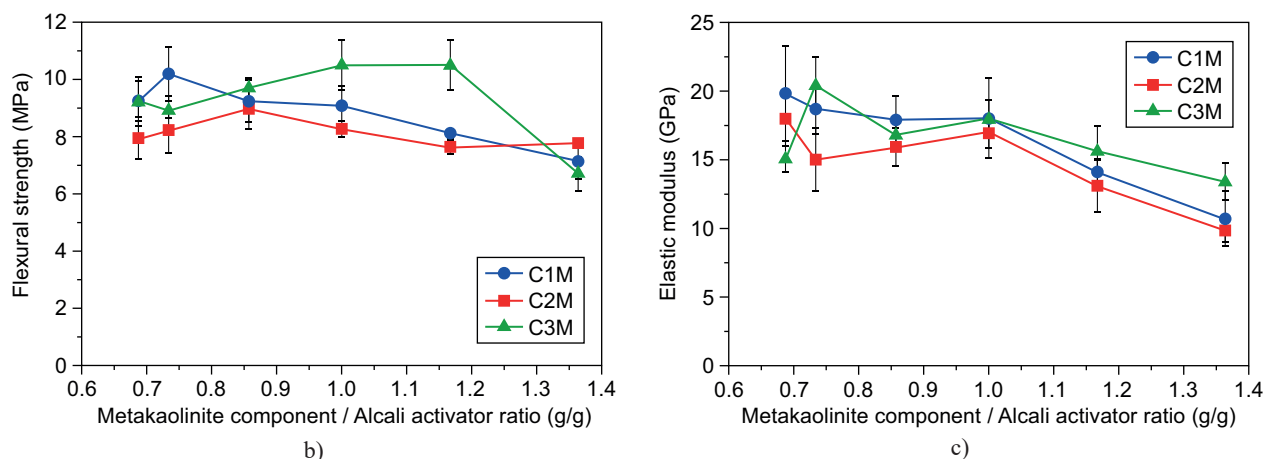
Figure 11. The influence of the meta-kaolinite components/alkali activator weight ratio on the flexural strength (b) and elastic modulus (c) of the filled geopolymers prepared from the C1M, C2M and C3M meta-kaolinite components. The error bars represent the standard deviation.

an Si:Al:Na molar ratio of 2:1:1 [4, 53]. This corresponds well with the results of the described experiments. The highest compressive strength of the geopolymer binders containing the C1M metakaolin was achieved with the G2 binder with an Si:Al:Na molar ratio of 2.11:1.0:1.14. The geopolymer based on the G3 binder with an Si:Al:Na molar ratio of 2.0:1.0:0.98 had a compressive strength only slightly lower (Table 2, Figure 11). An optimal composition of the geopolymer binders prepared by the alkali activation of the thermally treated kaolinitic claystones has not been published yet and should be the subject of further research. The optimal composition, in this case, will be probably different from the cited Si:Al:Na molar ratio of 2:1:1, because the chemical compositions of the kaolin and kaolinite claystones can be significantly different. This was also indicated by the results of this work (Table 1). Among the binders with the C2M processed kaolinitic claystone content, the highest compressive strength was achieved with the G9 binder at the Si:Al:Na ratio of 1.61:1.0:0.87.

CONCLUSIONS

Three clay materials (one kaolin a two kaolinitic claystones) were dehydrated at 750 °C, ground and classified. The results of the analysis of the raw materials, calcinates and dehydrated and ground clays resulted in the following conclusions:

- All the starting clay materials had a high content of kaolinite.
- The kaolinitic claystones contained more impurities than the kaolin, which resulted in their more intense shading.
- The kaolinite plates in the claystones were significantly smaller and less ordered than the plates in the kaolin.

- The kaolin had a significantly higher pore volume and average pore diameter compared to the claystones.
- The differences in the properties of the kaolin and claystones were maintained or increased during calcination and grinding.

The prepared aluminosilicate powder materials were blended in the required proportions with an alkali activator and supplemented with water to achieve its constant content in all the geopolymer binders. The geopolymers filled with inert particles (i.e., composites) were prepared by mixing the geopolymer binders with sand. The liquid binders, hardened binders and filled geopolymers were tested with the following results:

- The dynamic viscosities of the fresh geopolymer binders based on the treated kaolinitic claystones were significantly (3 ×) lower than the viscosities of the binders based on the treated kaolin.
- The dynamic viscosity decreased with the decreasing alkali activator content in the geopolymer binder.
- The intensity of the binder shades increased with the increasing content of the impurities (especially Fe_2O_3) present in the metakaolinite component.
- Both the pore volume and average pore diameter increased with the increasing content of the metakaolinite component in the geopolymer binders.
- The mechanical properties of all the prepared geopolymer composites were excellent up to a ratio of the metakaolinite component/alkali activator of 1:1, a further decrease in the alkali activator content led to a decrease in the compressive strength and modulus of elasticity.

The results of these experiments clearly indicate that the kaolinitic claystones are a promising raw material for the preparation of geopolymers. Their advantage, compared to kaolin, is the lower price, and for a number

of applications, also a significantly lower viscosity of the geopolymer binders. On the contrary, the darker shades of those geopolymers may be considered a disadvantage.

REFERENCES

1. Davidovits J. (1989): Geopolymers and geopolymeric materials. Journal of Thermal Analysis, 35, 429-441. Doi:10.1007/BF01904446
2. Davidovits J. (2008). Geopolymer: Chemistry and Applications. Institut Géopolymère, Saint-Quentin.
3. Kuenzel C., Li L., Vandeperre L., Boccaccini A.R., Cheeseman C.R. (2014): Influence of sand on the mechanical properties of metakaolin geopolymers. Construction and Building Materials, 66, 442-446. Doi:10.1016/j.conbuildmat.2014.05.058
4. Duxson P., Mallicoat S.W., Lukey G.C., Kriven W.M., van Deventer J.S.J. (2007): The effect of alkali and Si/Al ratio on the development of mechanical properties of metakaolin-based geopolymers. Colloids and Surfaces A: Physicochemical and Engineering Aspects, 292, 8-20. Doi:10.1016/j.colsurfa.2006.05.044
5. Yao X., Zhang Z., Zhu H., Chen Y. (2009): Geopolymerization process of alkali–metakaolinite characterized by isothermal calorimetry. Thermochimica Acta, 493, 49-54. Doi:10.1016/j.tca.2009.04.002
6. Rowles M.R., O'Connor B.H. (2009): Chemical and Structural Microanalysis of Aluminosilicate Geopolymers Synthesized by Sodium Silicate Activation of Metakaolinite. Journal of the American Ceramic Society, 92, 2354-2361. Doi:10.1111/j.1551-2916.2009.03191.x
7. Subaer, van Riessen A. (2007): Thermo-mechanical and microstructural characterisation of sodium-poly(sialate-siloxo) (Na-PSS) geopolymers. Journal of Materials Science, 42, 3117-3123. Doi:10.1007/s10853-006-0522-9
8. Duxson P., Provis J.L., Lukey G.C., Mallicoat S.W., Kriven W.M., van Deventer J.S.J. (2005): Understanding the relationship between geopolymer composition, micro-structure and mechanical properties. Colloids and Surfaces A: Physicochemical and Engineering Aspects, 269, 47-58. Doi:10.1016/j.colsurfa.2005.06.060
9. Wang H., Li H., Yan F. (2005): Synthesis and mechanical properties of metakaolinite-based geopolymer. Colloids and Surfaces A: Physicochemical and Engineering Aspects, 268, 1-6. Doi:10.1016/j.colsurfa.2005.01.016
10. Cheng T.W., Chiu J.P. (2003): Fire-resistant geopolymer produced by granulated blast furnace slag. Minerals Engineering, 16, 205-210. Doi:10.1016/s0892-6875(03)00008-6
11. Zhang Z., Wang H., Provis J.L., Bullen F., Reid A., Zhu Y. (2012): Quantitative kinetic and structural analysis of geopolymers. Part 1. The activation of metakaolin with sodium hydroxide. Thermochimica Acta, 539, 23-33. Doi:10.1016/j.tca.2012.03.021
12. Chen C., Gong W., Lutze W., Pegg I.L. (2011): Kinetics of fly ash geopolymerization. Journal of Materials Science, 46, 3073-3083. Doi:10.1007/s10853-010-5186-9
13. Lemougna P.N., MacKenzie K.J.D., Melo U.F.C. (2011): Synthesis and thermal properties of inorganic polymers (geopolymers) for structural and refractory applications from volcanic ash. Ceramics International, 37, 3011-3018. Doi:10.1016/j.ceramint.2011.05.002
14. Lemougna P.N., Chinje Melo U.F., Delplancke M.-P., Rahier H. (2013): Influence of the activating solution composition on the stability and thermo-mechanical properties of inorganic polymers (geopolymers) from volcanic ash. Construction and Building Materials, 48, 278-286. Doi:10.1016/j.conbuildmat.2013.06.089
15. Okada K., Ooyama A., Isobe T., Kameshima Y., Nakajima A., MacKenzie K.J.D. (2009): Water retention properties of porous geopolymers for use in cooling applications. Journal of the European Ceramic Society, 29, 1917-1923. Doi:10.1016/j.jeurceramsoc.2008.11.006
16. Aliabdo A.A., Abd Elmoaty A.E.M., Salem H.A. (2016): Effect of water addition, plasticizer and alkaline solution constitution on fly ash based geopolymer concrete performance. Construction and Building Materials, 121, 694-703. Doi:10.1016/j.conbuildmat.2016.06.062
17. Xie J., Kayali O. (2014): Effect of initial water content and curing moisture conditions on the development of fly ash-based geopolymers in heat and ambient temperature. Construction and Building Materials, 67, 20-28. Doi:10.1016/j.conbuildmat.2013.10.047
18. Kuenzel C., Vandeperre L.J., Donatello S., Boccaccini A.R., Cheeseman C., Brown P. (2012): Ambient Temperature Drying Shrinkage and Cracking in Metakaolin-Based Geopolymers. Journal of the American Ceramic Society, 95, 3270-3277. Doi:10.1111/j.1551-2916.2012.05380.x
19. Lizcano M., Gonzalez A., Basu S., Lozano K., Radovic M., Viehland D. (2012): Effects of Water Content and Chemical Composition on Structural Properties of Alkaline Activated Metakaolin-Based Geopolymers. Journal of the American Ceramic Society, 95, 2169-2177. Doi:10.1111/j.1551-2916.2012.05184.x
20. Aredes F.G.M., Campos T.M.B., Machado J.P.B., Sakane K.K., Thim G.P., Brunelli D.D. (2015): Effect of cure temperature on the formation of metakaolinite-based geopolymer. Ceramics International, 41, 7302-7311. Doi:10.1016/j.ceramint.2015.02.022
21. Perera D.S., Uchida O., Vance E.R., Finnie K.S. (2007): Influence of curing schedule on the integrity of geo-

polymers. Journal of Materials Science, 42, 3099-3106. Doi:10.1007/s10853-006-0533-6

22. Lancellotti I., Catauro M., Ponzoni C., Bollino F., Leonelli C. (2013): Inorganic polymers from alkali activation of metakaolin: Effect of setting and curing on structure. Journal of Solid State Chemistry, 200, 341-348. Doi:10.1016/j.jssc.2013.02.003

23. Rovnaník P. (2010): Effect of curing temperature on the development of hard structure of metakaolin-based geopolymer. Construction and Building Materials, 24, 1176-1183. Doi:10.1016/j.conbuildmat.2009.12.023

24. Ouellet-Plamondon C., Aranda P., Favier A., Habert G., van Damme H., Ruiz-Hitzky E. (2015): The Maya blue nanostructured material concept applied to colouring geopolymers. RSC Adv., 5, 98834-98841. Doi:10.1039/c5ra14076e

25. Puligilla S., Mondal P. (2013): Role of slag in microstructural development and hardening of fly ash-slag geopolymer. Cement and Concrete Research, 43, 70-80. Doi:10.1016/j.cemconres.2012.10.004

26. Pacheco-Torgal F., Moura D., Ding Y., Jalali S. (2011): Composition, strength and workability of alkali-activated metakaolin based mortars. Construction and Building Materials, 25, 3732-3745. Doi:10.1016/j.conbuildmat.2011.04.017

27. Nematollahi B., Sanjayan J. (2014): Effect of different superplasticizers and activator combinations on workability and strength of fly ash based geopolymer. Materials & Design, 57, 667-672. Doi:10.1016/j.matdes.2014.01.064

28. Huiskes D.M.A., Keulen A., Yu Q.L., Brouwers H.J.H. (2016): Design and performance evaluation of ultralightweight geopolymer concrete. Materials & Design, 89, 516-526. Doi:10.1016/j.matdes.2015.09.167

29. Zhang Z., Wang K., Mo B., Li X., Cui X. (2015): Preparation and characterization of a reflective and heat insulative coating based on geopolymers. Energy and Buildings, 87, 220-225. Doi:10.1016/j.enbuild.2014.11.028

30. Medri V., Fabbri S., Ruffini A., Dedecek J., Vaccari A. (2011): SiC-based refractory paints prepared with alkali aluminosilicate binders. Journal of the European Ceramic Society, 31, 2155-2165. Doi:10.1016/j.jeurceramsoc.2011.05.006

31. Nematollahi B., Sanjayan J., Shaikh F.U.A. (2016): Matrix design of strain hardening fiber reinforced engineered geopolymer composite. Composites Part B: Engineering, 89, 253-265. Doi:10.1016/j.compositesb.2015.11.039

32. Zhang H.-y., Kodur V., Cao L., Qi S.-l. (2014): Fiber Reinforced Geopolymers for Fire Resistance Applications. Procedia Engineering, 71, 153-158. Doi:10.1016/j.proeng.2014.04.022

33. Hanzlíček T., Steinerová M., Straka P., Perná I., Siegl P., Švarcová T. (2009): Reinforcement of the terracotta sculpture by geopolymer composite. Materials & Design, 30, 3229-3234. Doi:10.1016/j.matdes.2008.12.015

34. Sazama P., Bortnovsky O., Dědeček J., Tvarůžková Z., Sobalík Z. (2011): Geopolymer based catalysts – New group of catalytic materials. Catalysis Today, 164, 92-99. Doi:10.1016/j.cattod.2010.09.008

35. Alzeer M.I.M., MacKenzie K.J.D., Keyzers R.A. (2016): Porous aluminosilicate inorganic polymers (geopolymers): a new class of environmentally benign heterogeneous solid acid catalysts. Applied Catalysis A: General, 524, 173-181. Doi:10.1016/j.apcata.2016.06.024

36. Li L., Wang S., Zhu Z. (2006): Geopolymeric adsorbents

from fly ash for dye removal from aqueous solution. J Colloid Interface Sci, 300, 52-9. Doi:10.1016/j.jcis.2006.03.062

37. Mužek M.N., Svilović S., Zelić J. (2013): Fly ash-based geopolymeric adsorbent for copper ion removal from wastewater. Desalination and Water Treatment, 52, 2519-2526. Doi:10.1080/19443994.2013.792015

38. Perera D.S., Aly Z.,. Vance E.R, Mizumo M. (2005): Immobilization of Pb in a Geopolymer Matrix. Journal of the American Ceramic Society, 88, 2586-2588. Doi:10.1111/j.1551-2916.2005.00438.x

39. Hwang C.-L., Huynh T.-P. (2015): Effect of alkali-activator and rice husk ash content on strength development of fly ash and residual rice husk ash-based geopolymers. Construction and Building Materials, 101, 1-9. Doi:10.1016/j.conbuildmat.2015.10.025

40. Khater H.M. (2012): Effect of Calcium on Geopolymerization of Aluminosilicate Wastes. Journal of Materials in Civil Engineering, 24, 92-101. Doi:10.1061/(asce)mt.1943-5533.0000352

41. Nematollahi B., Sanjayan J., Shaikh F.U.A. (2015): Synthesis of heat and ambient cured one-part geopolymer mixes with different grades of sodium silicate. Ceramics International, 41, 5696-5704. Doi:10.1016/j.ceramint.2014.12.154

42. Duxson P., Fernández-Jiménez A., Provis J.L., Lukey G.C., Palomo A., van Deventer J.S.J. (2007): Geopolymer technology: the current state of the art. Journal of Materials Science, 42, 2917-2933. Doi:10.1007/s10853-006-0637-z

43. Lemougna P.N., Wang K.-t., Tang Q., Melo U.C., Cui X.-m. (2016): Recent developments on inorganic polymers synthesis and applications. Ceramics International, 42, 15142-15159. Doi:10.1016/j.ceramint.2016.07.027

44. Sabir B.B., Wild S., Bai J. (2001): Metakaolin and calcined clays as pozzolans for concrete: a review. Cement and concrete composites, 23, 441-454. Doi:10.1016/S0958-9465(00)00092-5

45. Ozer I., Soyer-Uzun S. (2015): Relations between the structural characteristics and compressive strength in metakaolin based geopolymers with different molar Si/Al ratios. Ceramics International, 41, 10192-10198. Doi:10.1016/j.ceramint.2015.04.125

46. Frost R.L., Vassallo A.M. (1996): The dehydroxylation of the kaolinite clay minerals using infrared emission spectroscopy. Clays and Clay Minerals, 44, 635-651. Doi:10.1346/CCMN.1996.0440506

47. Tironi A., Trezza M.A., Scian A.N., Irassar E.F. (2012): Kaolinitic calcined clays: Factors affecting its performance as pozzolans. Construction and Building Materials, 28, 276-281. Doi:10.1016/j.conbuildmat.2011.08.064

48. Madejová J., Komadel P. (2001): Baseline studies of the clay minerals society source clays: infrared methods. Clays and Clay Minerals, 49, 410-432. Doi:10.1346/CCMN.2001.0490508

49. Hoch M., Bandara A. (2005): Determination of the adsorption process of tributyltin (TBT) and monobutyltin (MBT) onto kaolinite surface using Fourier transform infrared (FTIR) spectroscopy. Colloids and Surfaces A: Physicochemical and Engineering Aspects, 253, 117-124. Doi:10.1016/j.colsurfa.2004.10.118

50. Arab P.B., Araújo T.P., Pejon O.J. (2015): Identification of clay minerals in mixtures subjected to differential thermal and thermogravimetry analyses and methylene

blue adsorption tests. Applied Clay Science, 114, 133-140. Doi:10.1016/j.clay.2015.05.020

51. Ptáček P., Opravil T., Šoukal F., Wasserbauer J., Másilko J., Baráček J. (2013): The influence of structure order on the kinetics of dehydroxylation of kaolinite. Journal of the European Ceramic Society, 33, 2793-2799. Doi:10.1016/j.jeurceramsoc.2013.04.033

52. Yip C.K., Provis J.L., Lukey G.C., van Deventer J.S.J. (2008): Carbonate mineral addition to metakaolin-based geopolymers. Cement and Concrete Composites, 30, 979-985. Doi:10.1016/j.cemconcomp.2008.07.004

53. Kuenzel C., Neville T.P., Donatello S., Vandeperre L., Boccaccini A.R., Cheeseman C.R. (2013): Influence of metakaolin characteristics on the mechanical properties of geopolymers. Applied Clay Science, 83-84, 308-314. Doi:10.1016/j.clay.2013.08.023

54. Autef A., Joussein E., Gasgnier G., Pronier S., Sobrados I., Sanz J., Rossignol S. (2013): Role of metakaolin dehydroxylation in geopolymer synthesis. Powder Technology, 250, 33-39. Doi:10.1016/j.powtec.2013.09.022

55. Escalera E., Antti M.L., Odén M. (2012): Thermal treatment and phase formation in kaolinite and illite based clays from tropical regions of Bolivia. IOP Conference Series: Materials Science and Engineering, 31, 012017. Doi:10.1088/1757-899x/31/1/012017

56. Krieger I.M., Dougherty T.J. (1959): A Mechanism for Non-Newtonian Flow in Suspensions of Rigid Spheres. Transactions of the Society of Rheology, 3, 137-152. Doi:10.1122/1.548848

57. Panagiotopoulou C., Kontori E., Perraki T., Kakali G. (2006): Dissolution of aluminosilicate minerals and by-products in alkaline media. Journal of Materials Science, 42, 2967-2973. Doi:10.1007/s10853-006-0531-8

58. Latella B.A., Perera D.S., Durce D., Mehrtens E.G., Davis J. (2008): Mechanical properties of metakaolin-based geopolymers with molar ratios of $Si/Al \approx 2$ and $Na/Al \approx 1$. Journal of Materials Science, 43, 2693-2699. Doi:10.1007/s10853-007-2412-1

59. Pelisser F., Guerrino E.L., Menger M., Michel M.D., Labrincha J.A. (2013): Micromechanical characterization of metakaolin-based geopolymers. Construction and Building Materials, 49, 547-553. Doi:10.1016/j.conbuildmat.2013.08.081

60. Yip C.K., Lukey G.C., Provis J.L., van Deventer J.S.J. (2008): Effect of calcium silicate sources on geopolymerisation. Cement and Concrete Research, 38, 554-564. Doi:10.1016/j.cemconres.2007.11.001